INDONESIAN JOURNAL ON GEOSCIENCE
Geological Agency
Ministry of Energy and Mineral Resources

Journal homepage: http://ijog.geologi.esdm.go.id
ISSN 2355-9314, e-ISSN 2355-9306

Quaternary Deposit Response to Earthquakes in Pemalang City Based on Peak Ground Acceleration, Earthquake Intensity, and Microtremor Method

Urip Nurwijayanto Prabowo[1], Sehah[1], Akmal Ferdiyan[1], and Sismanto[2]

[1]Department of Physics, Universitas Jenderal Soedirman
Jalan Dr. Suparno No. 61, Purwokerto 53123, Indonesia
[2]Department of Physics, Universitas Gajah Mada
Sekip Utara Bulaksumur, Yogyakarta, Indonesia

Corresponding author: urip.np@unsoed.ac.id
Manuscript received: May, 15, 2022; revised: March, 14, 2023;
approved: November, 11, 2023; available online: November, 23, 2023

Abstract - The northern part of Pemalang City consists of Quaternary deposits, having the potential for earthquake amplification effect. This amplification effect amplifies the ground shaking because of an earthquake (the local site effect) that has the potential to cause damage. This study investigated the amplification factor from the HVSR curve of microtremor measurements due to soil response based on ground shear strain, the risk level of the earthquake based on peak ground acceleration (PGA), and earthquake intensity. The microtremor data from five locations in Pemalang were used to calculate the amplification factor and predominant frequency. The damaging earthquake parameters around Java during 2010-2020 were used to calculate the PGA. The microtremor data were processed using the HVSR method, and PGA was calculated using the Kanai equation. The HVSR result shows that Pemalang has an amplification factor ranging from 6.23 to 19.59 and ground shear strain varying between 0.86 x 10^{-4} and 6.67 x 10^{-4}, which shows that Pemalang only experiences the vibration when an earthquake occurs. The PGA results using the Kanai equation (19.71-54.56 gal) were included in the low vulnerability category, and MMI earthquake intensity (3.08-4.70) was included in the felt earthquake category (II SIG BMKG scale). Therefore, the amplification factor from the HVSR curve of microtremor measurement, ranging from 6.23 to 19.59, showed low soil response and low-risk vulnerability based on the damaging earthquake parameter around Java during 2010-2020.

Keywords: peak ground acceleration, amplification, microtremor, PGA

How to cite this article:
Prabowo, U.N., Sehah, Ferdiyan, A., and Sismanto, 2023. Quaternary Deposit Response to Earthquakes in Pemalang City Based on Peak Ground Acceleration, Earthquake Intensity, and Microtremor Method. *Indonesian Journal on Geoscience*, 10 (3), p.407-417. DOI: 10.17014/ ijog-.10.3.407-417

Introduction

Background

The seismicity of Java Island is generally caused by the subduction of the Indo-Australian Plate beneath the Sunda Plate (Hutchings and Mooney, 2021). This subduction process also creates active inland faults on Java (Soehaimi, 2008). In Central and East Java, the intermediate and deep earthquakes (> 70 km) were caused by a plate subduction activity, with the seismic pattern predominantly distributed in the south of Java Island, such as in Kebumen, Yogyakarta, Pacitan, Malang, and Banyuwangi clusters (Muttaqy *et al*., 2023). While shallow earthquakes (< 70 km) are generally caused by activity from inland faults including Opak Fault, Kendeng Thrust Fault, and the Rembang-Madura-Kangean-Sakala (RMKS) Fault

Zones (Soehaimi, 2008; Muttaqy *et al*., 2023). The south part of Java shows seismic gaps that may be related to a potential source of megathrust earthquakes (Widiyantoro *et al*., 2020).

Pemalang and its surroundings are located in Central Java. Pemalang City centre is occupied by public and government facilities. This area as an economic growth region in Central Java is passed by the main routes of North Java Coast (Pantura). On September 16th, 2022, there was an earthquake in Pemalang with the magnitude of 2.7 on the Richter scale, the depth of 249 km, and the hypocentre position is at 7^0S and 109.27^0W (Hartono, 2022; Tim Detik Jateng, 2022). The earthquake was not destructive. The recorded seismic activities felt in Pemalang were the Kebumen earthquake on January 25th, 2014 (Yogaswara *et al*., 2020), and the Garut earthquake on December 3rd, 2022 (Putri, 2022). While the damaging earthquakes occurring around the Pemalang area were the Cilacap earthquake on April 4th, 2011; the Brebes earthquake on July 13th, 2013; the Kebumen earthquake on January 25th, 2014 (Yogaswara *et al*., 2020); and the Kalibening earthquake on April 18th, 2018 (Sipayung *et al*., 2019).

Geologically, Pemalang is occupied by Quaternary deposits, consisting of pebble, sand, silt, and clay as river and coastal deposits (Djuri *et al*., 1996). Because of the amplification effect, the Quaternary deposits are vulnerable to earthquake ground shaking. The earthquake ground shaking may result in a ground rupture damaging buildings. Nakamura *et al*. (2000) mention that areas suffering severe damage during an earthquake were Quaternary deposits (alluvial plains).

Pekalongan, which is located at the east of Pemalang, has a similar geological condition as Pemalang (Condon *et al*., 1996; Djuri *et al*., 1996). A research on Quaternary deposits of Pekalongan based on the HVSR curve of the microtremor analyses shows a high amplification factor (*A*) (Soehaimi *et al*., 2010). However, another research states that the amplification factor of the HVSR curve is different from earthquake amplification based on earthquake recording analysis (Hassani *et al*., 2011), empirical site characteristics (Satoh *et al*., 2001), and the other methods (Xu and Wang, 2021).

In this study, a seismic vulnerability analysis was carried out in the Quaternary deposits of Pemalang based on the value of the amplification factor and ground shear strain as the results of a microtremor analysis, peak ground acceleration (PGA), and earthquake intensity. A similar seismic vulnerability analysis using microtremor measurements and PGA has been carried out by other researchers in several other areas (Gurler *et al*., 1990; Konno and Ohmachi, 1998; Sulistiawan *et al*., 2017; Isburhan *et al*., 2019; Prabowo *et al*., 2019; Nakamura *et al*., 2000, Triyoso *et al*.).

The amplification factor from the microtremor was compared with the ground shear strain value to assess the relationship between the amplification factor and the soil response. Ground shear strain describes the ability of the soil layer to stretch and shift when experiencing an earthquake shaking (Yulianto *et al*., 2016). The level of earthquake damage is not only determined by the strength, duration, period of earthquake, and the distance, but also by the characteristics of the soil layer ability to respond to the vibration of the earthquake (geological conditions/local site effect) (Gurler *et al*., 1990).

The PGA calculated in this study is based on Fukushima Tanaka (PGA.f) and Kanai (PGA.k) equations. PGA.f was used as an additional parameter to calculate the ground shear strain. Whilst, the PGA.k was used to determine the risk level of the earthquake damage due to local site effects caused by Quaternary deposits, then compared with the amplification factor. The PGA.k adds a predominant period (inverse of predominant frequency) in the calculation, which describes the local site effect or geological characteristic of the area (Nakamura, 2000; Prabowo *et al*., 2019). The predominant frequency determined from the spectral ratio of the microtremor provided soil structure information to assess the soil amplification (Anggono *et al*., 2016). PGA.k was also used to calculate the earthquake intensity based on the Modified Mercalli Intensity (MMI) scale. The earthquake intensity is a scale

of earthquake strength on the surface of the earth that is qualitatively based on an observion on an earthquake impact.

Materials and Methods

The data used in this study are the microtremor and earthquake data shown in Figure 1. Microtremor is a constant vibration on the surface of the earth beside the earthquake (Aki, 1957). The source of microtremors are daily human activities and natural phenomena (rain, wind, ocean waves, *etc.*) (Okada, 2003). In this study, microtremor data analyses were derived from the measurement of five points in Pemalang using the M.A.E. seismometer (three components) with the duration of each measurement is 20 minutes and the data sampling interval is 4 mS. The portable GPS was used to determine the position of the measurement point.

Microtremor measurement data was processed using the Horizontal to Vertical Spectrum Ratio (HVSR) method. The data processing procedure follows the rules of SESAME (Site Effects Assessment using Ambient Excitations) (SESAME European Research Project, 2004). In the first step, stationary microtremor signals were manually selected by creating signal windows with the width of each window is 20 second. Stationary microtremor signals are signals that are not affected by noise in the form of earthquake and human activities. Advanced data processing does not use nonstationary signals.

Data selection in the time domain is changed into the spectrum domain through the Fast Fourier Transform (FFT) process with a 5% cosine taper, and subsequently smoothed using the Konno-Omachi algorithm with a constant b = 20 (Konno and Ohmachi, 1998). The spectrum of each signal component is compared based on the following equation (Nakamura, 1989):

$$HVSR = \frac{\sqrt{H_{EW}^2 + H_{NS}^2}}{V} \quad \text{..... (1)}$$

where:
HVSR is the HVSR ratio spectrum,
H_{EW} is a spectrum of horizontal components (east-west direction),
H_{NS} is a spectrum of horizontal components (north-south direction), and
V is the vertical components spectrum.

The HVSR ratio spectrum curve shows that the frequency of the curve peak is the dominant

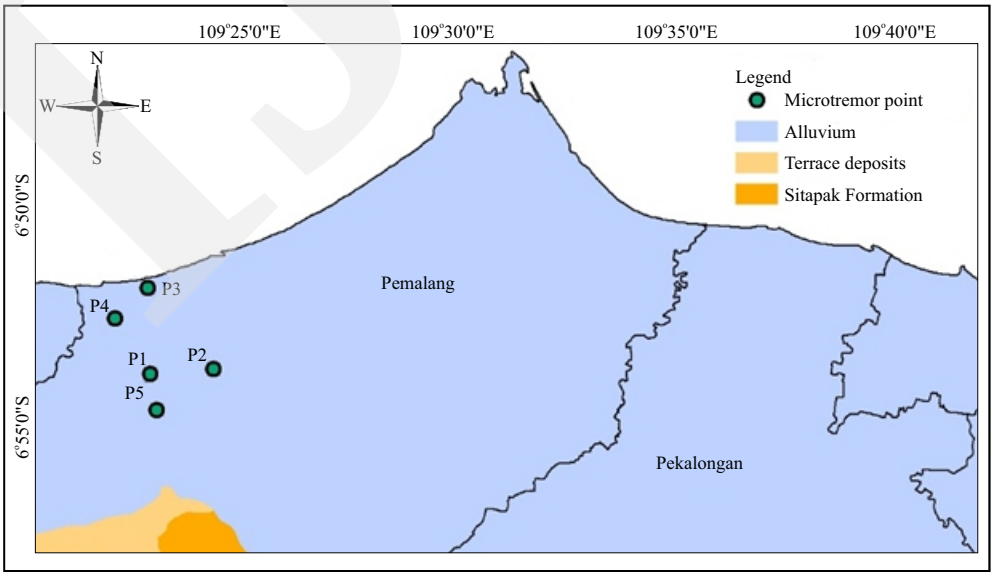

Figure 1. Microtremor measurement point map. Different colours stand for geological formation (modified from Djuri *et al.,* 1996 and Condon *et al.*, 1996).

frequency value (f_0), and the height of the curve peak is the amplification factor (A). The results of the HVSR spectrum ratio are curves that meet the criteria for reliable conditions (SESAME European Research Project, 2004).

The earthquake data used are the damaging earthquakes occurred in Java during the 2010 -2020 period (Yogaswara *et al*., 2020) with a magnitude greater than 4 SR (Table 1). The PGA calculation was carried out deterministically for all earthquake events in Table 1.

In this study, PGA calculations used the Fukushima-Tanaka (Fukushima and Tanaka, 1990) and Kanai (Douglas, 2018) Equations as follows:

$$\log PGA.f = 0,41M_s - \log\left\lfloor R + 0,033x10^{0,41MS}\right\rfloor - 0,00,4R + 1,28 \quad ....(2)$$

$$PGA.k = \frac{5}{\sqrt{T}}10^{\left[(0,6M)-\left(1,66+\frac{3,60}{R}\right)\log_{10}R+\left(0,167-\frac{1,83}{R}\right)\right]} \quad .....(3)$$

where:
PGA.f is the value of PGA (gal) using the Fukushima-Tanaka Equation 2
PGA.k is the value of PGA (gal) using the Kanai Equation 3,
T is the value of the predominant period (second) which has inversed value of predominant frequency (f_0),
M is the magnitude of the earthquake in SR,
M_S is the magnitude of surface wave, and
R is the hypocentre distance of the earthquake.

The magnitude conversion to calculate PGA used the equation from Tim Pusat Studi Gempa Nasional (2018). PGA calculations are classified based on Table 2 to determine the risk level of the earthquake in the studied area.

Earthquake intensity based on the Modified Mercalli Intensity (MMI) scale was calculated based on the following Equation 4 (Wald, 1999).

Table 1. Damaging Earthquakes Occurred in Java During the 2010-2020 period (Yogaswara *et al*., 2020)

No	Event	Earthquake Areas	Lat (deg)	Lon (deg)	Depth (km)	Magnitude (SR)
1	March 10, 2020	Sukabumi, West Java	-6,89	106,62	10	5.1
2	April 2, 2019	Sumenep. East Java	-7.24	114.6	10	5
3	Augst 2, 2019	Lebak, Banten	-7.54	104.58	10	7.4
4	Dec. 26, 2019	Sukabumi, West Java	-8.05	106.82	10	5
5	Jan. 23, 2018	Lebak, Banten	-7.21	105.91	10	6.4
6	April 18, 2018	Banjarnegara, Central Java	-7.21	109.65	4	4.4
7	June 13, 2018	Sumenep. East Java	-6.90	113.89	21	4.7
8	July 7, 2018	Lebak, Banten	-6.98	106.34	6	4.6
9	Oct. 10, 2018	Situbondo, East Java	-7.39	114.43	6	6.1
10	April 24, 2017	Tasikmalaya, West Java	-8.10	107.86	13	5.4
11	Dec. 15, 2017	Tasikmalaya, West Java	-7.75	108.11	107	6.9
12	Nov. 6, 2016	Pengalengan, West java	-7.25	107.54	10	4.2
13	Nov. 16, 2016	South coast, East Java	-9.32	113.12	69	6.2
14	June 25, 2015	Madiun, East Java	-7.73	111.69	10	4.2
15	Jan. 25, 2014	Kebumen, Central Java	-8.48	109.17	48	6.5
16	April 19, 2013	Banjarnegara, Central Java	-7.29	109.91	17.6	4.8
17	July 8, 2013	Malang, East Java	-9.10	113.00	9.44	5.9
18	July 13, 2013	Brebes, Central Java	-7.17	108.72	1.2	4.6
19	Dec. 18, 2013	Sukabumi, West Java	-6.87	106.81	10.9	4.3
20	June 4, 2012	Sukabumi, West Java	-7.91	106.24	52.86	5.7
21	Sept. 8, 2012	Bogor, West Java	-6.70	106.60	10	4.8
22	April 4, 2011	Cilacap, Central java	-10.01	107.69	10	7.1
23	June 12, 2011	Lebak, Banten	-7.01	106.30	10	4.9
24	August 28, 2011	Bandung, West Java	-8.16	107	18	4.9
25	Jan. 10, 2010	Garut, West Java	-8.02	107.91	14	5.4
26	Mei 18, 2010	Sukabumi, West Java	-8.22	107.21	13	6
27	June 26, 2010	Tasikmalaya, West Java	-8.37	107.98	34	6.3
28	August 21, 2010	Bantul, Yogyakarta	-8.03	110.30	10	5

Table 2. Classification of the Risk Level of Earthquake Damages According to BNPB Regulatory Chief No. 2 of 2012

Disaster	Risk Level Class		
	Low	Medium	High
Earthquake	PGA <0,250g	0,2501g < PGA < 0,70g	PGA > 0,701g

$$MMI = 3.66 \log PGA.k - 1.66 \quad \text{..... (4)}$$

The MMI value was then correlated with the BMKG scale intensity classification (Table 3) to give the qualitative interpretation of the MMI value.

The ground shear strain (γ) value is calculated using the Equations 5 and 6 (Nakamura, 1997):

$$\gamma = e\frac{PGA.f}{\pi^2 v_b}K_g \quad \text{..... (5)}$$

$$K_g = \frac{A^2}{f_0} \quad \text{.....(6)}$$

where:

K_g is the seismicity index (an index that describes the rates of ground surface susceptibility against deformation),

A and f_0 are the amplification factors and dominant frequency of microtremor measurement results.

The assumption used in Equation 5 is the efficiency of soil dynamic force (e) which is 60%, and the shear wave velocity value in the bedrock layer (v_b) is 600m/s. The ground shear strain (γ) value of the researched area was then classified based on Table 4.

Table 4. Strain Dependence of Soil Dynamic Properties (Nakamura, 1997)

Ground shear strain	10^{-6}	10^{-5}	10^{-4}	10^{-3}	10^{-2}	10^{-1}
Phenomena		Wave vibration		Crack, settlement	Landslide, soil compaction, liquefaction	
Dynamic Properties		Elastic		Elasto-plastic	Collapse	
					The repeated effect, loading speed effect	

Result and Discussion

The results of data processing in this study can be seen in Table 5. The sample of the HVSR result is shown in Figure 2.

Dominant Frequency and Amplification Factor of Microtremor Data

The dominant frequency of microtremor results ranges from 1.560 to 11.560 Hz (Figure 3), with the largest value in the south of the studied area (P5). The value of the dominant frequency reflected the thickness of the young sediment layer (Seht and Wohlenberg, 1999). Thus, based on the dominant frequency value, the Quaternary deposits are getting thicker from the south to the north, approaching the coast.

Table 3. IMM Value Interpretation Based on BMKG Scale Intensity (Musli *et al*., 2016)

MMI Scale	SIG BMKG Scale	Simple Description	Detailed Description	PGA (gal)
I–II	I	Not felt	Not felt or felt by some people, but recorded by a device.	<2,9
III–IV	II	Felt	Many people feels it, but it does not cause damage. Light objects hung swaying, and the glass windows shake.	2,9-88
V–VI	III	Minor damage	Nonstructural buildings have minor damage such as hair cracks on the walls, tiles shift down, and some fall.	89-167
VII–VIII	IV	Medium damage	Many cracks occurred on the walls of simple buildings, and some collapse with broken glass. Some plaster walls are loose. Most tiles shift down or fall. The structure of the buildings has minor to moderate damages.	168-564
IX–XII	V	Heavy damage	Most of the walls of permanent buildings collapse. The structure of the buildings suffers severe damage. Railroads arch.	>565

Table 5. Data Processing Results

Microtremor points	Long	Lat	*A*	f_0 (Hz)	K_g	*PGA.f* (gal)	*PGA.k* (gal)	MMI scale	γ (x10^{-4})
P1	109.39	-6.90	6.23	7.94	4.89	17.53	45.03	4.39	0.86
P2	109.41	-6.89	9.79	7.75	12.37	17.12	43.82	4.35	2.12
P3	109.38	-6.86	7.78	1.56	38.80	17.19	19.71	3.08	6.67
P4	109.37	-6.88	6.47	3.59	11.66	17.52	30.27	3.76	2.04
P5	109.39	-6.91	19.59	11.56	33.20	17.64	54.56	4.70	5.86

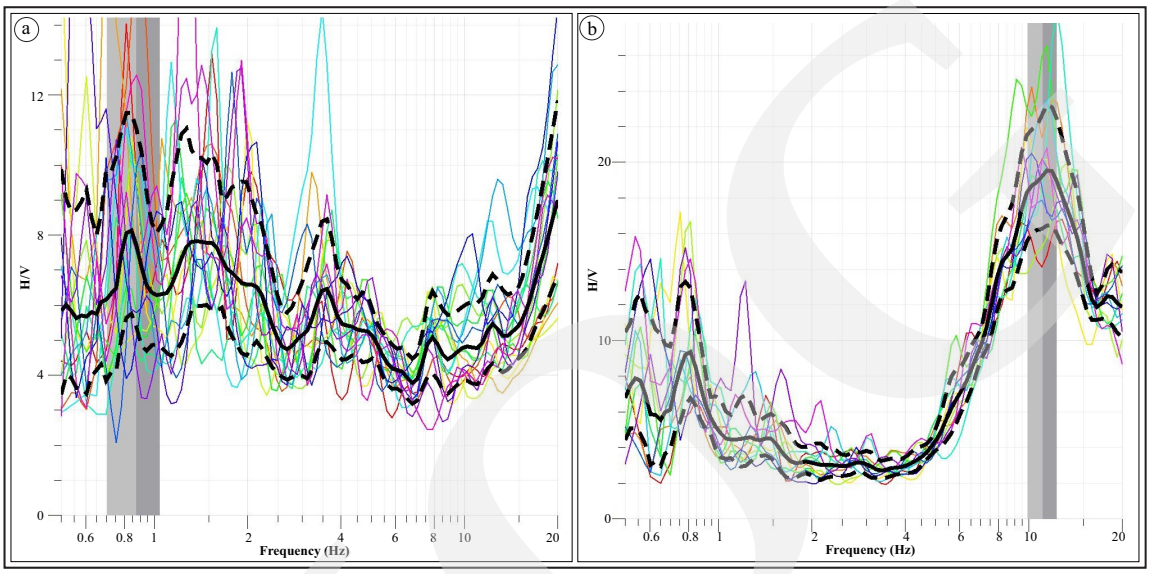

Figure 2. HVSR ratio spectrum curve – a) P4; b) P5.

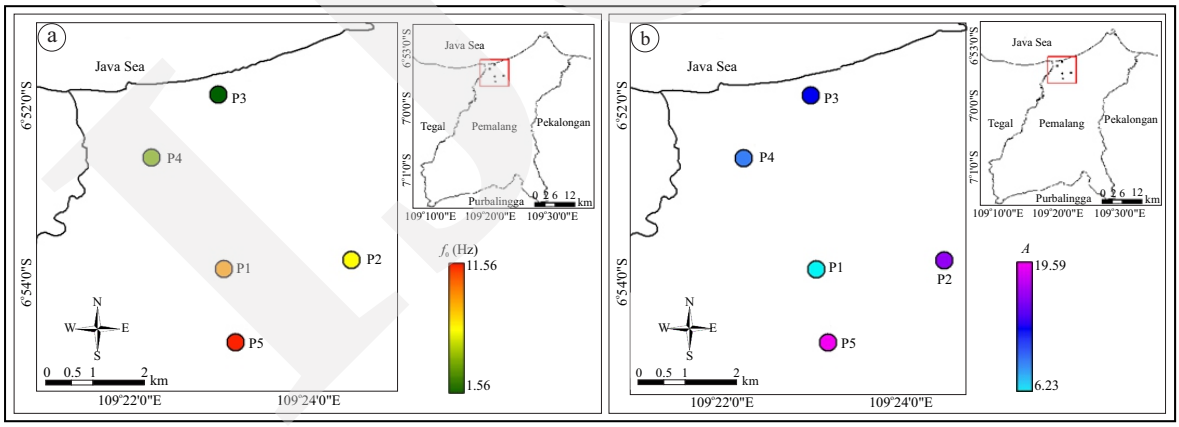

Figure 3. (a) Dominant frequency and (b) amplification factor of microtremor point.

The amplification factor (*A*) of the microtremor measurement results ranged from 6.230-19.59 (Figure 3) with the largest value in the south of the studied area (point P5). Nakamura *et al*. (2000) state that amplification factors describe the soil layer vibration of an earthquake that comes from bedrock (rock layers below). Thus, areas with higher amplification factors have a higher potential to damage during an earthquake (Nakamura *et al*., 2000). However, the amplification factor of the HVSR curve is different from the earthquake amplification based on earthquake recording

analysis (Hassani *et al*., 2011) and other methods (Xu and Wang, 2021). The amplification factor of the HVSR curve can not directly be used to derive the amplification factor, because the synthetic simulation shows that the HVSR peak is sensitive not only to the velocity contrast but also to Poisson's ratio of the sedimentary layer and the source-receiver distance (Lachet and Bard, 1995).

Peak Ground Acceleration (PGA) and Earthquake Intensity (IMM)

The PGA calculation results using the Kanai Equation (PGA.k) (Figure 4) are 19.71 - 54.56 gal, which belong to the low-risk level of earthquake damage category based on the classification in Table 2. The area with a greater PGA.k value has a higher risk of building damage due to earthquake ground shaking. Based on Equation 3 and Table 5, the frequency is proportional to the PGA.k value. Thinner sedimentary layers cause higher PGA.k values. It will experience a faster shock with a shorter duration if an earthquake occurs (Sari *et al*., 2006).

The earthquake intensity calculation in Pemalang shows a value of 3.08-4.70 on the Modified Mercally Intensity scale (Figure 4), which is included in the felt earthquake category based on Table 3. The PGA.k and earthquake intensity show a good correlation with the history of the earthquake in Pemalang, which shows that Pemalang has never suffered the severe damage due to earthquakes (Yogaswara *et al*., 2020). This result came from a calculation using a damaging earthquake occurred in Java during 2010–2020. Thus, more seismic event data (earthquakes) is needed for a further research.

Ground Shear Strain (γ)

The ground shear strain values range from 0.86 x 10^{-4} to 6.67 x 10^{-4} (Figure 5). Based on

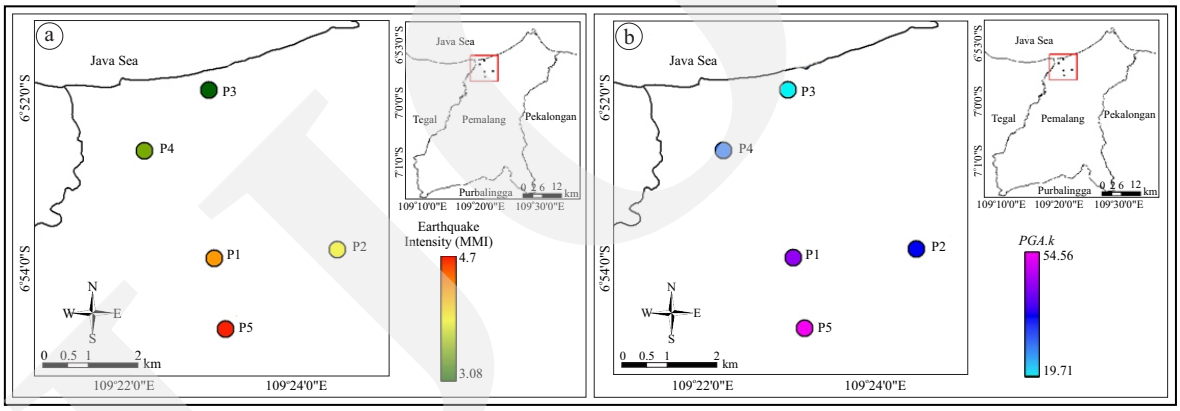

Figure 4. (a) Earthquake intensity and (b) *PGA.k* of microtremor point.

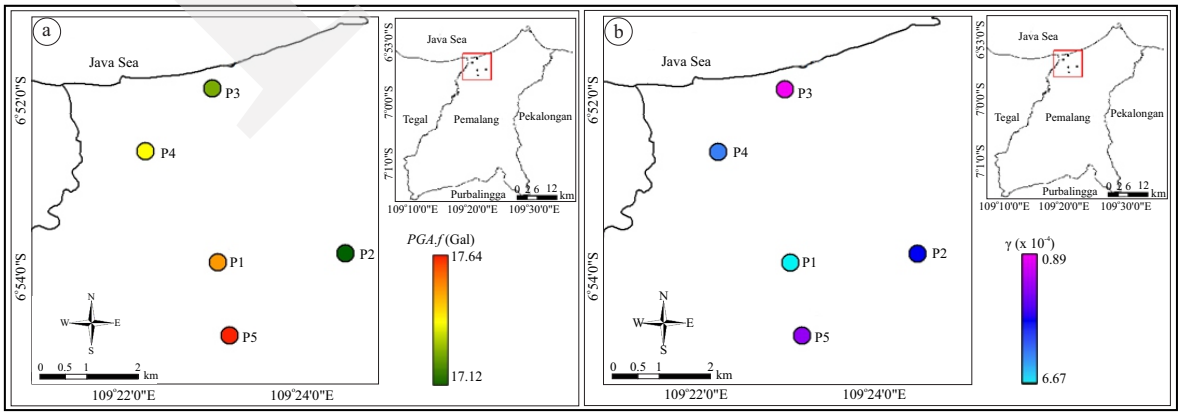

Figure 5. (a) *PGA.f* and (b) Ground Shear Strain (GSS) value of measurement point.

Table 4, the results of the ground shear strain show the studied area only experienced vibrations, there was no damage when an earthquake occurred. Based on Equation 5 and Table 5, the frequency is inversely proportional to the ground shear strain value. Areas with thick Quaternary deposits and low dominant frequency values are vulnerable to soil deformation (Haerudin *et al*., 2019).

The ground shear strain value is small due to the small PGA.f value (low magnitude earthquake or great distance from epicentre). This can be seen from the PGA.f value (17.12 - 17.64) included in the low category based on Table 2, but the seismic vulnerability index value (K_g) is quite large (4.888 - 38.80) following Equation 6. In comparison to the May 26th, 2006 earthquake in Yogyakarta, the damaged area had Kg= 14 and PGA.f= 375 gal. The high PGA.f value is due to the near epicentre and large magnitude of the May 26th, 2006 earthquake (Daryono *et al*., 2009).

The P3 measurement point located in the coastal area has the highest K_g. The Quaternary deposits of P3 are classified as sandy beach along the north coast of Java which consist of unconsolidated fine to medium sand, gray to blackish gray, and have low resistance to wave erosion and ocean currents (Solihuddin *et al*., 2021). Gurler *et al*. (1990) and Nakamura *et al*., (2000) assumed that the K_g was related to the weak point of the ground surface.

The PGA.k value and the ground shear strain value are different parameters in explaining the characteristics of the Quaternary deposits. The unconsolidated characteristics make Quaternary deposits experience the phenomenon of amplification and attenuation of waves when an earthquake passes through (Prabowo *et al.,* 2016). Thus, the value of PGA.k and ground shear strain may also be related to the earthquake amplification and attenuation.

The thin layer (the high frequency) of Quaternary deposits amplified earthquake waves and continued to the surface, so the PGA.k value becomes greater. Whereas on thick layers (the low frequency), the PGA value will be small due to the attenuation effect, while ground shear stress has the opposite properties. The ground shear strain value describes the effect of attenuation that absorbs the earthquake wave energy. Thus, the thicker the sediment layer, the greater the attenuation effect, and the greater energy absorbed by the layer. The thick and soft layers can not maintain their elastic properties, they will experience soil deformation (high ground shear strain value).

Conclusions

The Quaternary deposits in Pemalang comprise pebble, sand, silt, and clay as river and coastal deposits with amplification factors ranging from 6.23-19.59 resulting from the HVSR curve of the microtremor. This amplification factor range correlates with low soil deformation in the form of ground vibrations (low ground shear strain) and low-risk level of earthquake damage according to BNPB Regulatory (low value of PGA.k and low earthquake intensity). The use of amplification factors, resulting from microtremors in seismic vulnerability assessment and determination of the risk level of earthquake damages, requires further reviews. For example, correlating the amplification factor with an earthquake damage map at the studied area to determine the amplification limit value correlated with potential damage due to an earthquake.

The results showed the level of seismic activity felt in the Pemalang area was quite low, but caution and disaster mitigation efforts were needed using more comprehensive seismic data events around the Pemalang area due to the unconsolidated Quaternary deposits and fault around Pemalang.

Acknowledgement

The authors gratefully acknowledge the physics laboratory of Unnes Semarang for the seismometer used in this study

References

Aki, K., 1957. *Space and Time Spectra of Stationary Stochastic Waves, with Special Reference to Microtremors,* XXXV.

Anggono, T., Syuhada, Hananto, N.D., and Handayani, L., 2016. Site Response Characteristics of Simeulue Island, Indonesia as Inferred from H/V Spectral Ratio of Ambient Noise Records. *Journal of Mathematical and Fundamental Sciences*, 48 (2), p.130-142. DOI: 10.5614/j.math.fund.sci.2016.48.2.4.

Condon, W.H., Pardyanto, I., Ketner, K.B., Amin, T.C., Gafoer, S., and Samodra, H., 1996. *Geological Map of The Banjarnegara and Pekalongan Sheet, Java, scale 1:100.000*.

Daryono, Sutikno, Sartohadi, J., Dulbahri, and Brotopuspito, K.S., 2009. Efek Tapak Lokal (Local Site Effect) di Graben Bantul Berdasarkan Pengukuran Mikrotremor. *International Conference Earth Science and Technology*, p.4-9.

Djuri, M., Samodra, H., Amin, T.C., and Gafoer, S., 1996. *Geological Map of Purwokerto and Tegal Quadrangles, Java, scale 1:100.000*.

Douglas, J., 2018. *Ground motion prediction equations 1964*. Department of Civil and Environmental Engineering, University of Strathclyde.

Fukushima, Y. and Tanaka, T., 1990. A New Attenuation Relation for Peak Horizontal Acceleration of Strong Earthquake Ground Motion in Japan. *Bulletin of the Seismological Society of America*, 80, p.757-783.

Gurler, E.D., Nakamura, Y., Saita, J., and Sato, T., 1990. Local site effect of Mexico City based on microtremor measurement. *Proceedings of 6th International Conference of Seismic Zonation*.

Haerudin, N., Rustadi, Fitriawan, H., Siska, D., and Farid, M., 2019. Earthquake Disaster Mitigation Mapping By Modeling of Land Layer And Site Effect Zone. *Jurnal Ilmiah Pendidikan Fisika Al-Biruni*, 08 (1), p.53-67. DOI: 10.24042/jipfalbiruni. v8i1.3705.

Hartono, U., 2022. *Analisa BMKG Soal Gempa Darat Pemalang dan 13 Sesar Aktif di Jateng*. https://Www.Detik.Com/Jateng/Berita/d-6295393/Analisis-Bmkg-Soal-Gempa-Darat-Pemalang-Dan-13-Sesar-Aktif-Di-Jateng [September 16th].

Hassani, B., Zafarani, H., Farjoodi, J., and Ansari, A., 2011. Estimation of site amplification , attenuation and source spectra of S-waves in the East-Central Iran. *Soil Dynamics and Earthquake Engineering*, 31 (10), p.1397-1413. DOI: 10.1016/j.soildyn. 2011.05.017.

Hutchings, S.J. and Mooney, W.D., 2021. The Seismicity of Indonesia and Tectonic Implications. *Geochemistry, Geophysics, Geosystems*, 22 (9). DOI: 10.1029/ 2021GC009812

Isburhan, R.W.P., Nuraeni, G., Verdhora Ry, R., Yudistira, T., Cipta, A., and Cummins, P., 2019. Horizontal-to-Vertical Spectral Ratio (HVSR) Method for Earthquake Risk Determination of Jakarta City with Microtremor Data. *IOP Conference Series: Earth and Environmental Science*, 318 (1). DOI: 10.1088/1755-1315/318/1/012033.

Konno, K. and Ohmachi, T., 1998. Ground-Motion Characteristics Estimated from Spectral Ratio between Horizontal and Vertical Components of Microtremor. *Bulletin of the Seismological Society of America*, 88 (1), p.228-241.

Lachet, C. and Bard, P.Y., 1995. Theoretical Investigations on the Nakamura's Technique. *Proceedings of 3rd International Conference on Recent Advances in Geotechnical Earthquake Engineering and Soil Dynamics, St. Louis, Missouri*, p.671-675.

Musli, Masturyono, Murjaya, J., and Riyadi, M., 2016. Studi Awal Penyusunan Skala Intensitas Gempabumi badan Meteorologi Klimatologi dan Geofisika. *Jurnal Meteorologi Dan Geofisika*, 17 (2), p.89-100.

Muttaqy, F., Nugraha, A.D., Puspito, N.T., Sahara, D.P., Zulfakriza, Z., Rohadi, S., and Supendi, P., 2023. Double-difference earthquake relocation using waveform cross-correlation in Central and East Java, Indonesia. *Geoscience Letters*, 10 (1). DOI: 10.1186/s40562-022-00259-2.

Nakamura, Y., 1989. A Method for Dynamic Characteristics Estimation of Subsurface us-

ing Microtremor on the Ground Surface. *QR of RTRI*, 30 (1), p.25-33.

Nakamura, Y., 1997. Seismic Vulnerability Indices For Ground And Structures Using Microtremor. *World Congress on Railway Research, Florence*, p.1-7.

Nakamura, Y., 2000. Clear Identification of Fundamental Idea Of Nakamura'S. *Proceedings of XII World Conference Earthquake Engineering, New Zealand*.

Nakamura, Y., Sato, T., and Nishinaga, M., 2000. Local Site Effect Of Kobe Based On Microtremor. *Proceeding of the 6th International Conference on Seismic Zonation EERI,* Palm Springs California, p.3-8.

Okada, H., 2003. The Microtremor Survey Method. *In: Geophysical Monograph Series,* 12. Society of Exploration Geophysicists.

Prabowo, U.N., Amalia, A.F., and Budhi, W., 2019. Peak Ground Acceleration and Earthquake Intensity Microzonation in Watukumpul, Pemalang Regency. *Indonesian Journal of Science and Education*, 3 (2), p.60-65. DOI: 10.31002/ijose.v3i2.1169.

Prabowo, U.N., Marjiyono, and Sismanto, 2016. Amplifikasi dan atenuasi gelombang seismik di lapisan sedimen permukaan. *Sciencetech*, 2 (1), p.112-116.

Putri, N.A., 2022. *Gempa Bumi di Garut, Getaran Terasa Hingga Kabupaten Pemalang*. https://Pemalang.Inews.Id/Read/218336/Gempa-Bumi-Di-Garut-Getaran-Terasa-Hingga-Kabupaten-Pemalang [December 4]).

Sari, M.A., Wibowo, N.B., and Darmawan, D., 2006. Pemetaan Percepatan Getaran Tanah Maksimum Dan Intensitas Gempabumi Di Kawasan Jalur Sesar Sungai Oyo Yogyakarta. *Jurnal Fisika*, 6 (2), p.101-107.

Satoh, T., Kawase, H., and Ichi Matsushima, S., 2001. Differences Between Site Characteristics Obtained From Microtremors, S-waves, P-waves, and Codas. *Bulletin of the Seismological Society of America* (91).

Seht, M.I. and Wohlenberg, J., 1999. Microtremor Measurements Used to Map Thickness of Soft Sediments. *Bulletin of the Seismological Society of America*, 89 (1), p.250-259.

SESAME European Research Project, 2004. *Guidelines For The Implementation Of The H/V Spectral Ratio Technique On Ambient Vibrations Measurements, Processing And Interpretation*.

Sipayung, R., Sianipar, D., Prayoedhie, S., Daryono, Arifin, J., Simanjuntak, A.V.H., Muksin, U., Prabu, S., Daniarsyad, G., Haryanta, Putranto, N., and Azimi, A., 2019. Revisiting the 2018 Kalibening Earthquake Sequence in Central Java: Call for the Revision of Earthquake Hazard. *IOP Conference Series: Earth and Environmental Science*, 273 (1). DOI: 10.1088/1755-1315/273/1/012018.

Soehaimi, A., 2008. Seismotektonik dan Potensi Kegempaan Wilayah Jawa. *Jurnal Geologi Indonesia*, 3 (4), p.227-240.

Soehaimi, A., Marjiono, and Kamawan, 2010. Mikrozonasi Kerentanan Bahaya Goncangan Gempa Bumi Kota Pekalongan Berdasarkan Analisis Mikrotremor. *Jurnal Sumber Daya Geologi*, 20 (5), p.277-290.

Solihuddin, T., Husrin, S., Salim, H.L., Kepel, T.L., Mustikasari, E., Heriati, A., Ati, R. N.A., Purbani, D., Mbay, L.O.N., Indriasari, V.Y., and Berliana, B., 2021. Coastal erosion on the north coast of Java: Adaptation strategies and coastal management. *IOP Conference Series: Earth and Environmental Science*, 777 (1). DOI: 10.1088/1755-1315/777/1/012035.

Sulistiawan, H., Supriyadi, and Yulianti, I., 2017. Seismic Hazard Analysis Based on Earthquake Vulnerability and Peak Ground Acceleration using Microseismic Method at Universitas Negeri Semarang. *Journal of Physics: Conference Series*, 812, p.1-7. DOI: 10.1088/1742-6596/755/1/011001.

Tim Detik Jateng, 2022. *Gempa Darat M 2,7 Guncang Pemalang*. https://www.Detik.Com/Jateng/Berita/d-6289667/Gempa-Darat-m-27-Guncang-Pemalang [September 13th].

Tim Pusat Studi Gempa Nasional, 2018. *Peta sumber dan bahaya gempa Indonesia tahun*

2017. Pusat Penelitian dan Pengembangan Perumahan dan Permukiman (Indonesia).

Triyoso, W., Suwondo, A., and Naibaho, Z.Y.X., 20201. Earthquake Potential Hazard Analysis of PalembangCity, Sumatra Island. *Indonesian Journal on Geoscience*, 8 (1), p.1-9. DOI: 10.17014/ijog.8.1.1-9

Wald, 1999. *Relationships between Peak Ground Acceleration, Peak Ground Velocity and Modified Mercalli Intensity in California*. USGS.

Widiyantoro, S., Gunawan, E., Muhari, A., Rawlinson, N., Mori, J., Hanifa, N.R., Susilo, S., Supendi, P., Shiddiqi, H.A., Nugraha, A.D., and Putra, H.E., 2020. Implications for megathrust earthquakes and tsunamis from seismic gaps south of Java Indonesia. *Scientific Reports*, 10 (1). DOI: 10.1038/s41598-020-72142-z.

Xu, R. and Wang, L., 2021. The horizontal-to-vertical spectral ratio and its applications. *Eurasip Journal on Advances in Signal Processing*, 2021 (1). DOI: 10.1186/s13634-021-00765-z.

Yogaswara, D.S., Kriswinarso, T., Harvan, M., Hidayanti, Yatimantoro, T., Imananta, R.T., Ramdhan, M., Priyobudi, Rahayu, R.H., Simangunsong, G.B., Setiyono, U., Gunawan Indra, Hawati, P., Panjaitan, O., Anggraini, S., Apriani, M., and Julius, A.M., 2020. *Gempa Signifikan dan Merusak 1821 s.d Juni 2020* (Daryono, ed. of 1st ed.). Pusat Gempa dan Tsunami, Kedeputian Bidang Geofisika, BMKG.

Yulianto, G., Harmoko, U., and Widada, S., 2016. Identification of Potential Ground Motion Using the HVSR Ground Shear Strain Approach in Wirogomo Area, Banyubiru Subdistrict, Semarang Regency. *International Journal of Applied Environmental Sciences*, 11 (6), p.1497-1507.